JOURNAL OF MARINE SCIENCES & ENVIRONMENTAL TECHNOLOGIES
Vol. 10, Issue No. 2 (December-2025)
DOI: https://doi.org/10.59743/jmset.v10i2.185

ISSN (Print): 2413-5267
ISSN (Online): 2706-9966

Mixed Matrix Membranes-Derived from High-Density Polyethylene and *Mesembryanthemum Crystallinum* for Separation of Methylene Blue Dye from Aqueous Solutions

Almahdi A. Alhwaige[1,2,*], Ali N. Al-Drogi[1,3], Muammer B. Yahiya[1,4], Wael K. Elhrari[5]

[1]Department of Chemical and Petroleum Engineering, Faculty of Engineering Alkhoms, Elmergib University, Alkhoms, Libya
[2]Department of Chemical Engineering, Faculty of Engineering, University of Tripoli, Tripoli, Libya
[3]The National Oil Corporation, Tripoli, Libya
[4]The National Company for Cement Contribution, Alkhoms, Libya
[5]Libyan Polymer Research Center, Tajora, Tripoli

***E-mail:** a.alhwaige@uot.edu.ly

أغشية ذات مصفوفة مختلطة مشتقة من بولي إيثيلين عالي الكثافة والنبات الثلجي لفصل صبغة الميثيلين الزرقاء من المحاليل المائية

المهدي عطيه الحويج[1،2،*]، علي نوري الدروقي[1،3]، معمر بشير يحيى[1،4]، وائل خليفة الحراري[5]

[1]الهندسة الكيميائية والنفطية، كلية الهندسة الخمس، جامعة المرقب، الخمس، ليبيا
[2]الهندسة الكيميائية، كلية الهندسة، جامعة طرابلس، طرابلس، ليبيا
[3]المؤسسة الوطنية للنفط، طرابلس، ليبيا
[4]الشركة الأهلية المساهمة للإسمنت، الخمس، ليبيا
[5]المركز الليبي للدائن، تاجوراء، طرابلس، ليبيا

Received: 18 July 2025; Revised: 30 August 2025; Accepted: 10 September 2025

Abstract

The membrane technology has been found to play a significant role in water purification applications such as wastewater treatment and brackish water desalination. Mixed matrix membranes (MMMs) are a new type of promising membranes that derived from polymer matrixes and nanomaterials. The goal of this study is to develop a new type of MMMs from dispersion of *Mesembryanthemum crystallinum* (MC) in a polymeric matrix of high density polyethylene (HDPE). Three MMMs were fabricated, which classified according to the wt% MC content as HDPE-SC/MC-0, HDPE-SC/MC-1, and HDPE-SC/MC-2. The MMMs characteristics such as hydrophilicity, porosity, permeability, pure water flux have been studied. The performance of the obtained MMMs for rejection of methylene blue dye (MBD) also has been investigated. The results indicated that the addition of 2 wt% of MC in membrane enhanced the rejection efficiency of the neat HDPE membrane for MBD from 42 to 60 %.

Keywords: *High-density polyethylene, Membrane technology, Mixed matrix membrane, Industrial wastewater treatment, Methylene blue dye.*

الملخص

لقد وجد بأن تقنية الأغشية تلعب دورًا مهمًا في تطبيقات معالجة وتنقية المياه مثل معالجة مياه الصرف الصحي وتحلية المياه قليلة الملوحة ومياه البحر. أغشية المصفوفة المختلطة mixed matrix membrane (MMMs) هي فئة جديدة من الأغشية المصنعة عن طريق الجمع بين المواد البوليمرية والمواد النانوية، وهي تقجم حل مستقبلي لتحديات معالجة المياه. عليه، تهدف هذه الدراسة إلى تطوير نوع جديد من أغشية المصفوفة المختلطة (MMMs) من توزيع جسيمات النبات الثلجي (MC) *Mesembryanthemum crystallinum* في مصفوفة

بوليمرية من البولي إيثيلين عالي الكثافة (HDPE). فلقد تم تصنيع ثلاثة أنواع من MMMs، والتي تم تصنيفها وفقًا لمحتوى النسبة الوزنية لكمية MC في العينة: HDPE-SC/MC-0 و HDPE-SC/MC-1 و HDPE-SC/MC-2. حيث تشمل هذه الدراسة خصائص MMMs مثل خاصية المحبّة للماء والمسامية والنفاذية وتدفق الماء النقي. كما تم التحقق من أداء أغشية المصفوفة المختلطة (MMMs) التي تم إنتاجها لفصل صبغة الميثيلين الزرقاء (MBD). ولقد أشارت النتائج إلى أن إضافة 2% من وزن MC لغشاء بولي إيثيلين عالي الكثافة قد أدى إلى تحسين كفاءة فصل صبغة الميثيلين الزرقاء (MBD) بزيادة نسبة الفصل من 42 إلى 60%.

الكلمات الدالة: بولي إيثيلين عالي الكثافة، تقنية الأغشية، غشاء المصفوفة المختلطة، معالجة مياه الصرف الصناعي، صبغة الميثيلين الزرقاء.

1. Introduction

Separation processes are desirable to achieve products with high purities in different applications such as petroleum industry, gas processing, food industry, pharmaceutical manufacture, and environmental protection. In addition, to supply communities and industry with high-quality water, removal and recovery of valuable of toxic components from water effluent streams received significant attention (Wang *et al*., 2014). Therefore, various separation techniques such as distillation, extraction, precipitation, adsorption, crystallization, membrane separation, and ion exchange processes have been applied for water and water purifications (Ekrayem *et al.*, 2021; Wetzel, 2001).

In modern life, separation technologies with minimal waste, zero discharge, and low energy preservation have received significant interest over the world (Alhwaige *et al.*, 2024). Besides, membrane technology has been considered as an efficient separation technique compared to the other traditional separation methods (Roy and Singh, 2017; Strathmann *et al.*, 2016; and Wu *et al.*, 2023). Membrane separation technique has received great attention in many industrial fields, such as gas separation, water desalination, wastewater treatment, food, medicine, biotechnology, and pharmacy. The positive points of membrane technology over other separation methods are low energy consumption, simple process with high efficiency, environmentally friendly process, easily coupled with other processes, applied for variable operating parameters, no additives and chemicals needed, and wide range of applications. In addition, low energy requirement, flexibility of operation, and abundant of raw materials contribute to membrane uses in both personal and industrial activates (Swamy *et al.*, 2013; and Zheng *et al*, 2015).

A membrane is a thin semipermeable sheet of material that separates molecules when a driving force is applied (Jhaveri and Murthy, 2016). The mechanism of most membrane processes is the selective filtration of one or more components from feed flow streams via permeation through pores with different sizes due to applying a pressure-driven force. The major challenge on the membrane research is fabrication of novel cost-effective membranes from eco-friendly raw materials with high flux and separation efficiency (Qu *et al.*, 2013).

Development of novel eco-friendly membranes with low fouling, high permeability, and excellent selectivity using sustainable materials is a major research interest for industry, academia, and national research centres. In addition, membranes structures play a major role in the performance of the permeation flux and separation efficiency. Therefore, the membranes have been categorized mainly into two types, symmetric and asymmetric membranes (Warsinger *et al.*, 2018). Neat polymeric membranes have several properties and permeation issues, which limit their applications as overall separation performance. Recently, mixed matrix membranes (MMMs) have been developed as an efficient approach to improve

the separation performance of polymer-based membranes. The MMMs consist of a polymer matrix as the continuous phase and nanoparticles as the dispersed phase, resulting excellent barrier properties can be achieved due to synergistic effects of both properties of polymer and dispersed phase. The majority of MMMs have been derived using embedded with 50−1000 nm size fillers and the resulting MMMs have been employed to design various MMMs for separation applications (Katare and Mandal, 2023; Liu *et al.*, 2024; and Wu *et al.*, 2023).

MMMs are one class of nanocomposite membranes that contains nanoparticles embedded in polymeric matrixes, results an enhancement in membrane uniformity, economically, and transport properties. The previous findings indicated that the importance of the proper choice of the single-phase and continuous matrix phase play a significant role on membranes transport characteristics. Thus, MMMs provide excellent transport characteristics of the inter-area of membrane, which is the important factor to the fabrication of perfect materials matrixes (Strathmann *et al.*, 2016). Therefore, MMMs is considered the alternative materials for use in water purification applications instead of the neat polymeric membranes (Lin *et al.*, 2014).

Nowadays, membrane separation techniques play a significant step in water purification (Zheng *et al.*, 2015). In addition, membrane technology utilizations in industrial wastewater effluents have sharply increased, mainly in steel factories, petrochemical industries, and stations of electric power generation due to their performance for wide pollutants rejection (Figoli and Criscuoli, 2017; Lin *et al.*, 2014; Mahajan and Koros, 2004; Strathmann *et al.*, 2016; and Swamy *et al.*, 2013). Therefore, polymer-based membranes have been employed to separate colloids and dissolved materials from water in various practical wastewater treatment processes (Mahajan and Koros, 2004). Such water pollutants are inorganic compounds (e.g., heavy metals), organics (e.g., dyes and hydrocarbons), and microorganisms (e.g., viruses) have been separated from water streams using membrane technology (Figoli and Criscuoli, 2017; and Swamy *et al.*, 2013). In Libya, the membrane technology has been applied for water desalination and removing unwanted impurities from the drinking water since thirty years ago. The first membrane technology has been established in Libya is Tajoura seawater desalination plant (Ezzeghni and El-Bourawi, 2016). In addition, there are many membrane systems have been used to treat underground water for human drinking.

Various abundant polymers have been used for fabrication of membranes toward high efficient rejection of pollutants from water and wastewaters (Warsinger *et al.*, 2018). Among these polymers, high-density polyethylene (HDPE) based membranes are widely used for water treatment due to its outstanding properties including high density, good thermal stability, oxidative resistance, and possesses high mechanical integrity. Moreover, it is insoluble in most of wastewater systems, working at wide temperatures, excellent pH tolerance, and has good dimensional stability (Lloyd *et al.*, 1990). Various membrane have been derived from HDPE plastic waste and they were used for removal of water pollutants from water effluents (Zukimin *et al.* 2017; Zulfiani *et al.*, 2023; and Zulfiani *et al.*, 2024). In addition, combination of HDPE with other polymers have showed a synergy of both polymers properties on membranes performance (Zulfiani *et al.*, 2023). However, the addition of additives such as natural waste materials to the HDPE matrix is still under investigation due to their compatibility (Zulfiani *et al.*, 2024). Therefore, in this research, utilization of HDPE waste polymer as a continuous polymeric matrix for development of a new class of MMMs, which derived from disperse of biomass particles in HDPE matrix. In addition, the obtained MMMs have been examined for elemination of methylene blue dye (MBD) from aqueous solutions.

Agricultural materials are a promising source for development various biomasses, which have been considered as cost effective material for wastewater treatment, which ascribed to availability of various reactive moieties like carboxyl, hydroxyl and hydroxyl, and phosphates functional groups. These groups are the most active sites for many pollutants such as heavy metal ions, toxic dyes, and hydrocarbons. Among of these biomass materials, maize cob waste, almond shell, sunflower seed hull, and wood sawdust have been evaluated for wastewater treatment applications (Lok *et al.*, 2017; and Nam and Park, 1999). *Mesembryanthemum crystallinum (Cryophytum crystallinum)* is a family aizoaceae. In addition, *Mesembryanthemum crystallinum* (MC) is a creeping plant, which called ice plant because it riches with ice on its leaves (see Figure 1). It is a flat, moist, and halophyte plant, which native to various regions including Africa and Sinai and southern Europe. In addition, it is naturalized in North America, South America, and Australia. Early, MC has been commonly utilized in the traditional medicine. In addition, MC has been examined for adsorption of MBD from aqueous solutions. The results indicated that MC has fast kinetics toward MBD with high efficiency (Abushaina *et al.*, 2018).

Figure 1. Optical image of *Mesembryanthemum crystallinum*.

2. Experimental Section

2.1. Materials

High-density polyethylene (HDPE) (melt flow index 0.05 g/10 min at 190 °C and 2.16 Kg ISO 1133, and value of density is 952 kg/m^3 ISO 1183) was supplied from SABIC Saudi Arabia, di-n-butyl phthalate (DNBP) 99%) was purchased from Alfa Aesar A Johnson Matthey Company, sodium chloride (NaCl) was obtained from Eurostar Scientific Ltd, and methylene blue dye (MBD) was used as an organic pollutant model. *Mesembryanthemum crystallinum* (MC) is a plant that was collected from the native biotope in Zliten, Libya (see Figure 1).

2.2. Synthesis of HDPE/Di-N-Butyl Phthalate Membrane

For the preparation of flat plate HDPE-DNBP membrane, 20 g of HDPE was mixed with 10 mL of DNBP, which was used as a plasticizer, and the mixture was heated at a temperature of 200 ^{o}C until a homogeneous mixture was formed. And then, the resultant mixture was cooled at 4 °C using an ice-water bath. The obtained membrane was made via the thermal method as

follows: A sample of HDPE-DNBP mixture was placed in the thermal piston at 200 ^{o}C, and then a pressure in the range from 0.5 bar to 2 bar was applied. Subsequently, the membrane was quickly taken from the thermal piston and placed in a water bath at room temperature to cool. Consequently, the DNBP was extracted from the membrane using isopropanol for 24 h. Thus, the high-density polyethylene/di-n-butyl phthalate membrane was obtained, which was abbreviated as HDPE-DNBP.

2.3. Synthesis of HDPE/Sodium Chloride Membrane

The HDPE/sodium chloride membrane was prepared using the similar method that described in the previous section with small modification. HDPE (20 g) was mixed with 10 g sodium chloride (NaCl, which abbreviated as SC), and then the mixture was heated at a temperature of 200 ^{o}C until a homogeneous mixture was formed. After that, the mixture was cooled at 4 °C using an ice-water bath. The membrane was derived using the thermal method as follows: A sample of HDPE and NaCl mixture was placed in the thermal piston at 200 ^{o}C, and then a pressure in the range from 0.5 bar to 2 bar was applied. Subsequently, the membrane was taken from the thermal piston quickly and placed in a water bath at room temperature to cool. And then, the NaCl was extracted using distilled water-bath for 24 h. Thus, the high-density polyethylene/sodium chloride membrane was obtained, which was abbreviated as HDPE-SC-MC-0.

2.4. Synthesis of HDPE/MC) Mixed Membrane

A new flat-plate membranes have been parathion using extrusion-molding method. In the first stage, specific quantities of HDPE and NaCl were together mixed with various proportions (0.5, 1.0, and 2.0) of MC and the obtained mixture was perfectly grind. In the second stage, the obtained mixture was blended using an extrusion at 200 °C, above the fusion/point-melting of HDPE, to form a homogeneous HDPE-SC mixed matrix of composites. The mixed matrix membrane (MMM) was fabricated as described in the previous section. The obtained MMMs have been abbreviated as HDPE-SC-MC-*x*, where *x* is represented the composition weight percentage of MC in the membrane (see Table 1).

Table 1. The membrane abbreviations and the starting materials contents.

Sample code	***Contents (wt%)***		
	HDPE	***NaCl***	***MC***
HDPE-SC/MC-0	90	10	0
HDPE-SC/MC-1	89	10	1
HDPE-SC/MC-2	88	10	2

2.5. Characterizations of the Obtained Membranes

Fourier infrared spectroscopy (FTIR) was used to investigate the chemical structure of MC. Fourier a Bruker Vertex infrared spectroscopy with resolution of 3 $cm^{-1}$and in the range of 4000-500 cm^{-1} was used in this study. The FT-IR measurements was evaluated using the KBr pellet procedure. Dry species of the MC samples were powdered in a mortar and a specific amount of sample was mixed with KBr, and then the KBr pellets were formed.

Contact angle measurement was performed to investigate the surface properties of the obtained MMMs. The contact angle of the prepared films was measured using a ramè-hart instrument co. model 200-F4. The contact angle goniometry of a captured image of a static drop of water 3 µL sitting on the membrane dried surface was measured at ambient conditions. To obtain average values, three measurements were performed at different locations on the surface of the membrane and average value of contact angles was calculated.

In the present study, the porosity of the obtained membranes was also measured according to wet and dry weights of the membrane as given in Eq.1 (Ghaemi and Khodakarami, 2019). However, this method is based on the assumption of complete saturation and the method may not account for closed pores.

$$\varepsilon\% = \frac{W_w - W_d}{\rho_w A \delta_o} \times 100 \qquad (1)$$

where the W_w and W_d are the weights of the wet and dry membrane (kg), respectively, δ_o is the thickness of the membrane (m), ρ_w is the density of the pure water (kg/m^3), and A is the membrane area (m^2).

2.6. Membrane Process

2.6.1. Membrane Process Set-up

The performance of the obtained membranes was assessed using a laboratory scale of membrane process, which equipped with a circular cell. Figure 2 shows a schematic diagram of the used membrane system. In this study, the permeate flow in membrane system provided a circular effective membrane surface area of 16.42 cm^2.

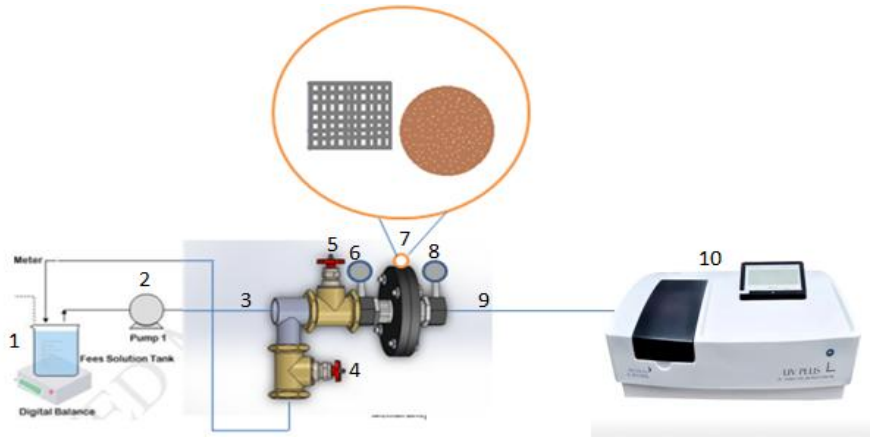

1. Tank, 2. Pump, 3. Flow rate in, 4. Valve in, 5. Valve Bottom discharge, 6. Pressure gage in let, 7. Membrane support, 8. Pressure gauge outlet, 9. Flow rate out, Ultra-volatile visible spectrophotometer (UV-vis).

Figure 2. A schematic diagram illustrations of the used experimental set-up.

2.6.2. Measurements of Membrane Flux and Permeability

The permeability measurement was obtained experimentally as follows: various volumetric flow rate as a function of applied pressure was obtained. The membrane has been placed in the unit and then, it was closed tightly. After opening the valve for bottom discharge, the pump was switched on to make sure that it was working perfectly. Then, the discharge valve was closed gradually until the water pressure reached to the required pressure. The discharge valve was lifted a little open to avoid the phenomenon of concentration polarization. Subsequently, various volumes (V) as a function of time (t) were collected at different applied pressures. The volumetric flow rate (Q) was calculated from the ratio of collected volume (V) and time interval (Δt); whereas the flux was calculated using the Eq. 2 (Saedi *et al.*, 2013):

$$J_A = \frac{Q}{A} \quad (2)$$

where: J_A, Q and A are the flux (L/m^2.h), volumetric flow rate of the permeated water (L/h), the effective area of membrane permeation (m^2), respectively.

In addition, the pressure drop was estimated from the difference between the feed and permeate pressures. The permeability value (P_M) for each membrane was evaluated from the slope of a straight-line of a plot the flux versus the pressure drop (Ghaemi and Khodakarami, 2019; and Saedi *et al.*, 2013).

$$J_A = P_M \times \Delta P \quad (3)$$

where P_M, J_A and ΔP are the permeability of the membrane (L/m^2.h.atm), the flux (L/m^2.h), and the pressure drop (atm), respectively.

2.6.3. The Membrane Rejection Efficiency of Methylene Blue Dye

In the first stage, a standard solution of methylene blue dye (MBD) was prepared with an initially concentration of 500 mg/L, which was obtained by dissolving 2.5 g of MBD in a volume of 5 L of distilled water. The required initial concentrations were obtained via diliution of the a specific amount of the previously prepared stock solution via adding a calculated volume of the distilled water to a specific volume of the standard solution according to the Eq. 4 (Salima *et al.*, 2012).

$$C_1 \times V_1 = C_2 \times V_2 \quad (4)$$

where C_1, V_1 are the required concentration of MBD solution (mg.L^{-1}), the needed volume of distilled water (L), respectively. C_2, V_2 are the properties of the stock solution.

In the second stage, the membrane efficacy for the MBD removal from wastewaters, MBD rejection test was carried out using the membrane process as shown in Figure 2. The MMM was inserted in the system and the experiment was carried out at ambient temperature. The membranes were conditioned in distilled water for 24 h before filtration, and then the MBD solution was processed the membrane. To investigate the effect of MC content in the Membrane composition, the separation experiments were evaluated form samples containing different MC content (HDPE-SC/MC-0, HDPE-SC/MC-2, and HDPE-SC/MC-3). For each experiment, several samples were collected at different processing time intervals. The absorbance of MBD solution of each sample was evaluated using ultra-volatile visible spectrophotometer (UV-vis) at wavelength of 664 cm^{-1}. Therefore, the MBD concentration in

each sample was obtained using the absorbance/concentration relationship on the previously prepared calibration curve (Saedi *et al.* 2013). The membrane efficiency for rejection of MB dye from water for each obtained MMM was obtained at various processing time interval as described in Eq. 5:

$$\eta\% = \left(1 - \frac{C_P}{C_F}\right) \times 100 \quad (5)$$

where η is the MB dye rejection efficiency (%). The C_F and C_P are, the feed and permeate MB dye concentrations (mg/L), respectively. The concentration of MBD was measured using a UV-vis spectrophotometer (Zulfiani, *et al.*, 2023).

3. Results and Discussion

3.1. Analysis of FT-IR

FT-IR is one of the most important characteristics that are calculated for preparation of polymeric membranes. Figure 3. In the FTIR spectra of MC, the broad peak at 3426 cm^{-1} is due to the stretching band of hydroxyl functional groups (–OH). The peaks at 2935 and 2848 cm^{-1} present the stretching vibration of the –C=H band (Alhwaige *et al.* 2013). The absorption bands located around 1634 cm^{-1} is ascribed to stretching vibration of the carbonyl groups (–C=O). The peaks at 1316 and 1018 cm^{-1} are could be corresponded respectively to the stretching modes of C-N (Abushaina *et al.*, 2018; and Salima *et al.*, 2012). The results indicated the MC is rich with –OH functional groups, which are important active site for removal MB dye (Ekrayem *et al.*, 2021).

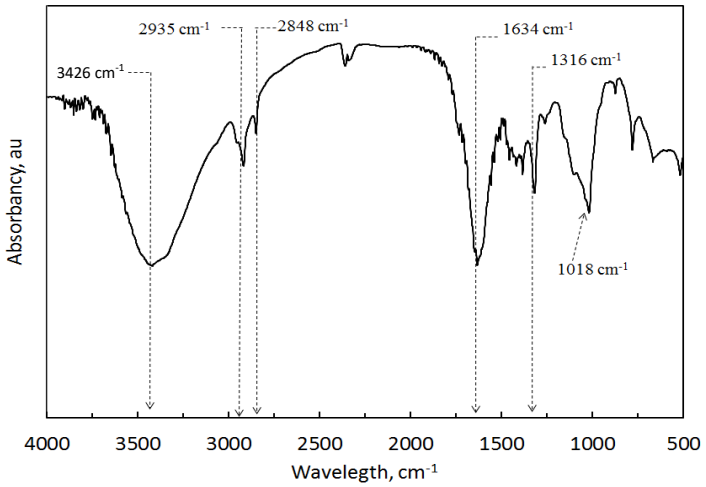

Figure 3. FTIR of *Mesembryanthemum Crystallinum*.

3.2. Analysis of Contact Angle

Surface property is one of the primary characteristics of membranes, and to know the properties of these membranes whether hydrophilic or hydrophobic nature. If the contact angle is less than 90º, the membrane surface is like water. If the contact angle is greater than 90º, the surface of the membrane is less wet with water. The contact angle is one of the most important membranes characteristics, which studied the wettability of the membrane surface

using liquid water (Alhwaige *et al.*, 2019). Figure 4 demonstrates of the average static contact angle results of the obtained membranes. The contact angle value of the neat membrane (HDPE-CS-MC-0) was slightly hydrophobic (θ>90^o); however, it is become hydrophilic after addition of MC-biobased particles (HDPE-CS-MC-1 and HDPE-CS-MC-3). As shown in Figure 4, the surface modification of the neat membrane with addition of MC indicated that it decreased from 91.6 of neat membrane HDPE-SC/MC-0 to 79.5 and 73.8 for HDPE-SC/MC-1 and HDPE-SC/MC-2, respectively. The decrease in the contact angle values is ascribed to the present of the MC-biobased particles. In other words, the increase of polymer concentration led to an increase in the contact angle of the membrane (Ajari *et al*, 2019). Therefore, the average static contact angle values demonstrated that the surface of the MC-based mixed matrix membranes (HDPE-SC/MC-1 and HDPE-SC/MC-2) were hydrophilic nature, which is preferred for membranes in water purification applications (Tolba *et al.*,2016).

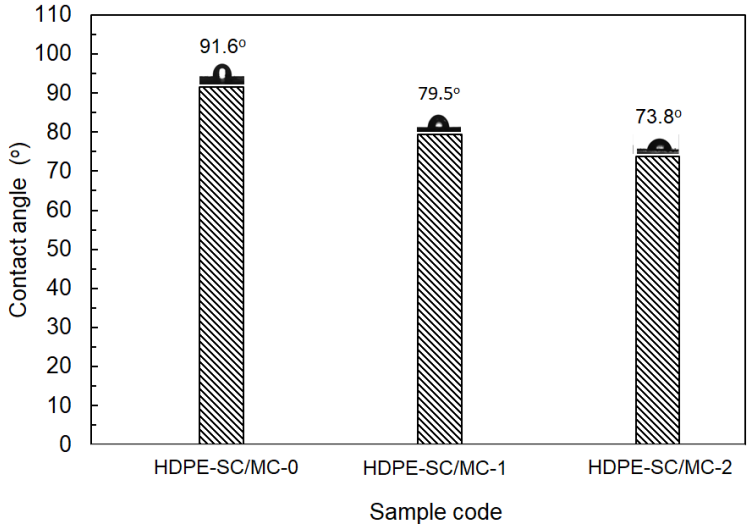

Figure 4: The images and contact angle values of the prepared mixed matrix membranes.

3.3. Porosity of the Membranes

Membrane porosity is one key of the membrane permeate flux and separation efficiency. Therefore, effect of MC-biobased particles on the porosity of the prepared MMMs was a part of the present study and the obtained results are demonstrated in Table 2. The addition of MC-biobased particles to the membrane matrix led to MMMs with high porosity as compared to the neat membrane (HDPE-SC/MC-0). The results indicated that all membranes have porosity between 15% and 30%. The porosity of the neat HDPE-SC/MC-0 membrane was 15.4%. The addition of MC-biobased particles into the matrix enhanced the membrane porosity. For example, the addition of 2 wt% MC-biobased particles to the neat membrane showed an increase ~50% in the porosity (HDPE-SC/MC-0). In addition, the HDPE-SC/MC-1 membrane has the highest porosity value as compared to the other membranes. The increase in the porosity of the MMMs is due to phase separation and porosity of the MC-biobased particles (Ghazanfari *et al.*, 2017).

Table 2. The properties of the obtained mixed matrix membranes.

Sample code	*Porosity (%)*	*Permeability (L/m²-h-atm)*	*Flux (L/m²-h)*
HDPE-SC/MC-0	15.4	724	1186
HDPE-SC/MC-1	30.0	N/A*	N/A*
HDPE-SC/MC-2	20.3	1138	1990

**N/A: Not Available.*

3.4. Microstructure of the Membrane surface

The optical light microscope is one of the most important characteristics and tests of membranes. The most important feature is that it is used to investigate the porosities and morphological properties of membranes. Figure 5 shows microstructure of the obtained HDPE-SC/MC-1 membrane. The results indicated that the membrane of HDPE-1 has a homogeneous surface with uniform pore structure. It suggested that the forming pores is due to elimination of sodium chloride nanoparticles via extraction after the membrane fabrication (Zulfian *et al.*, 2023). In addition, the images indicated that there are no agglomerations of the CM particles on the membrane surface. These investigations are positive points for the obtained MMMs.

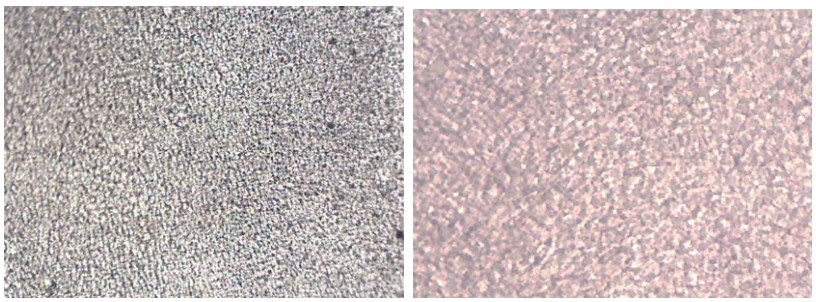

Figure 5. The microstructure of the HDPE-SC/MC-1 mixed matrix membrane.

3.5. Effect of Pressure on Membrane Permeate Flux

Particularly, applied pressure is found to be the most important parameter in the membrane processes. Thus, the effect of applied pressure on the membranes permeate fluxes was investigated. Figure 6 shows the permeate fluxes versus the applied pressure drop values (ΔP) for the fabricated MMMs. The results indicated that all the MMMs showed a similar behavior. The permeate flux (J_A) increased with an increase in the applied pressure drop (ΔP). For example, in the membrane HDPE-SC/MC-0, the permeate flux increased from 723.51 to 1137.64 L/m^2-h with a rise in the applied pressure drop from 0.987 to 1.85 atm. In addition, MC-based nanoparticles have a significant role for increasing the permeate flux. At the applied pressure drop of 2.16, the permeate flux of the HDPE-SC/MC-0 increased from 1186.36 to 1990.26 L/m^2-h with addition 1% MC-based nanoparticles (i.e. HDPE-SC/MC-1), which due to the increase in porosity as compared to the other membranes (see Table 2).

However, a reduction in the permeate flux (1474.4 L/m^2-h) was observed for the HDPE-SC/MC-2 membrane at similar conditions. These findings are in a good agreement with the previous studies (Zulfian *et al.*, 2023).

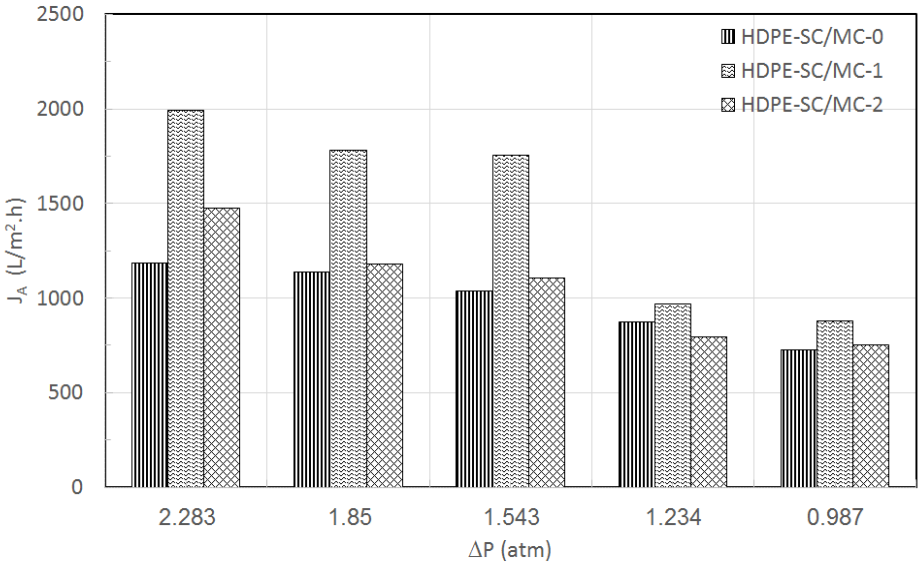

Figure 6. Effect of applied pressure on the membrane flux.

3.6. Measurement of the Membrane Permeability

Permeability factor is one of the important characteristics of any developed membranes, because it controls the effluent quantity. Therefore, measurements of the membranes permeabilities were a apart of this study. The permeability values of the fabricated membranes were obtained as described in Eq. 3. Figure 7 illustrates the slope of the plot of flux against applied pressure drop for each membrane. The results showed that the flux has a linear relationship with pressure drop for all obtained membranes. In addition, the membrane containing HDPE-SC/MC-1 has higher slope compared to the neat HDPE-SC-0 and HDPE-SC/MC-2. As seen in Figure 8, these observations indicated that the HDPE-SC/MC-1 has a maximum permeability value than the other membranes, which ascribed to the increase in the porosity. In terms of the pure water permeability, the permeability of neat HDPE membrane was increased from 288 to 833 L/m^2-h-atm. Therefore, it is interesting to report that MC enhances the permeability of the neat membrane (HDPE-SC/MC-0). This increase is due to the increase in the porosity as previously discussed. Similar observations for improvement of membrane permeability with addition of nanoparticle to polymer matrix have been previously reported (Ghaemi and Khodakarami, 2019).

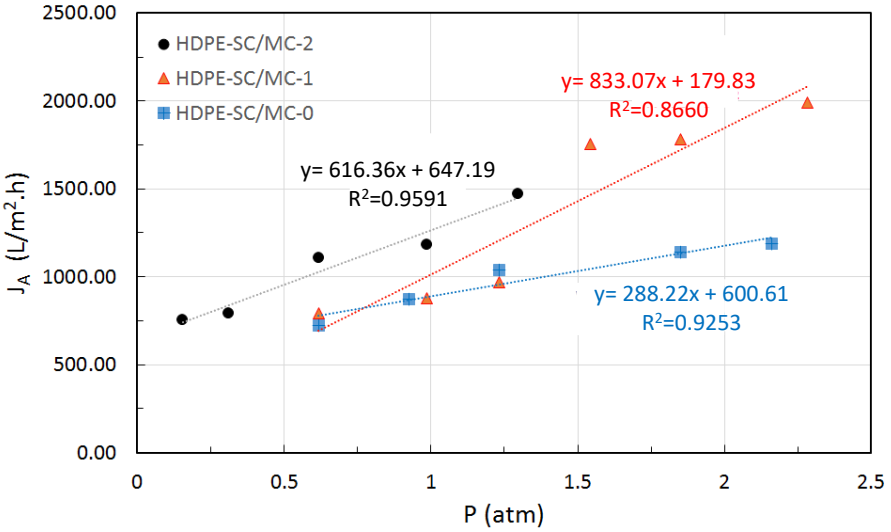

Figure 7. Pure water permeability of the obtained membranes.

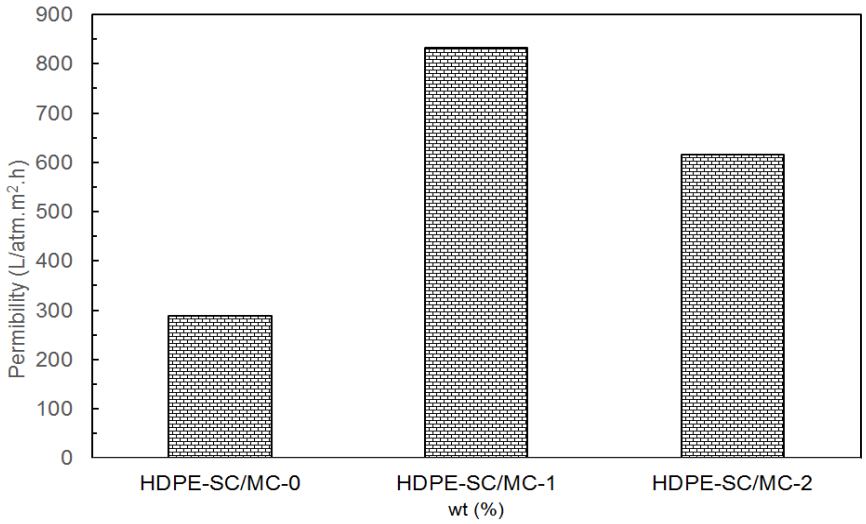

Figure 8. The permeability of the obtained membranes after 1 h.

3.7. The Permeation Fluxes of the HDPE-based MMMs

Figure 9 shows the permeate flux (J_A) of the HDPE-based membranes as a function of processing time before and after the addition of MC. The J_A values of the obtained membranes were measured at a constant pressure for each experiment. All the fluxes of the MMMs showed similar behaviors for reduction in J_A values with time. The J_A values of the MMMs were fast during the beginning, and then became slower which continued to decline over time. For example, the permeate fluxes of HDPE-SC/MC-1 and HDPE-SC/MC-2 membranes decreased from 256 and 226 L/m^2-h to 208 and 212 L/m^2-h, respectively, after the increase in the processing time from 0.405 h to 0.75 h. These observations are in consistent with the reported studies (Ghaemi and Khodakarami, 2019).

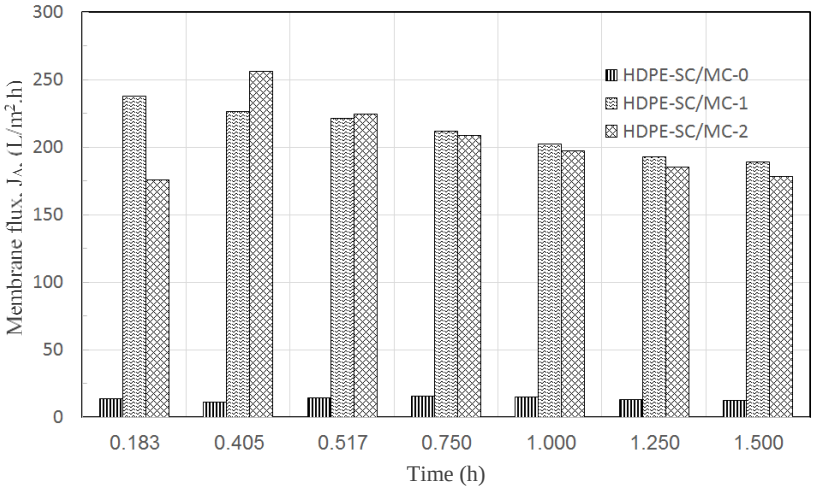

Figure 9. Effect of processing time on the membrane permeate flux.

In addition, the flux of HDPE-SC/MC-2 was faster than HDPE-SC/MC-1 at beginning; however, opposite observation was found after certain minutes. This change in behavior of permeation flux for HDPE-MC-2 was ascribed to the closing of some pores because they were narrowed, which were not tolerated to transport fluid through the membrane despite the persistence of pressure. In addition, the nanoparticle content decreased the permeate performance due to nanoparticles agglomerations and a decrease in the membrane porosity. While, in the case of HDPE-SC/MC-1 membrane, the pores were sufficient to transport liquid through the membrane with a small-continued decline in the flux at fixed pressure.

3.8. The Membrane Performance for Methylene Blue Dye Removal

3.8.1. *Calibration Curve*

Before the investigation of the membrane rejection efficiency of MB dye, the maximum wavelength (λ) for MB dye was obtained as well as the calibration curve. The maximum wavelength (λ) for MB dye was obtained using measurement of UV-vis absorbance for MB dye solution at various wavelengths. Figure 10a demonstrates the UV-vis absorbance for MB dye versus wavelength (λ). The results show the maximum wavelength (λ) at peak 664 nm. Therefore, at this wavelength (λ = 664 nm), the UV-vis spectrophotometer will be used to measurement the absorbance for MB dye during to preparation of the calibration curve.

The calibration curve was obtained by measuring UV-vis absorbance at different concentrations of MB dye in range from 10 to 2.5 mg L^{-1} MB dye, which were obtained via dilution of the previously prepared stock solution (50 mg L^{-1}). UV-vis absorbance for each concentration was measured at wavelength (λ) 664 nm. Figure 10b show the calibration curve of plot of UV-vis absorbance versus the concentration of MB dye.

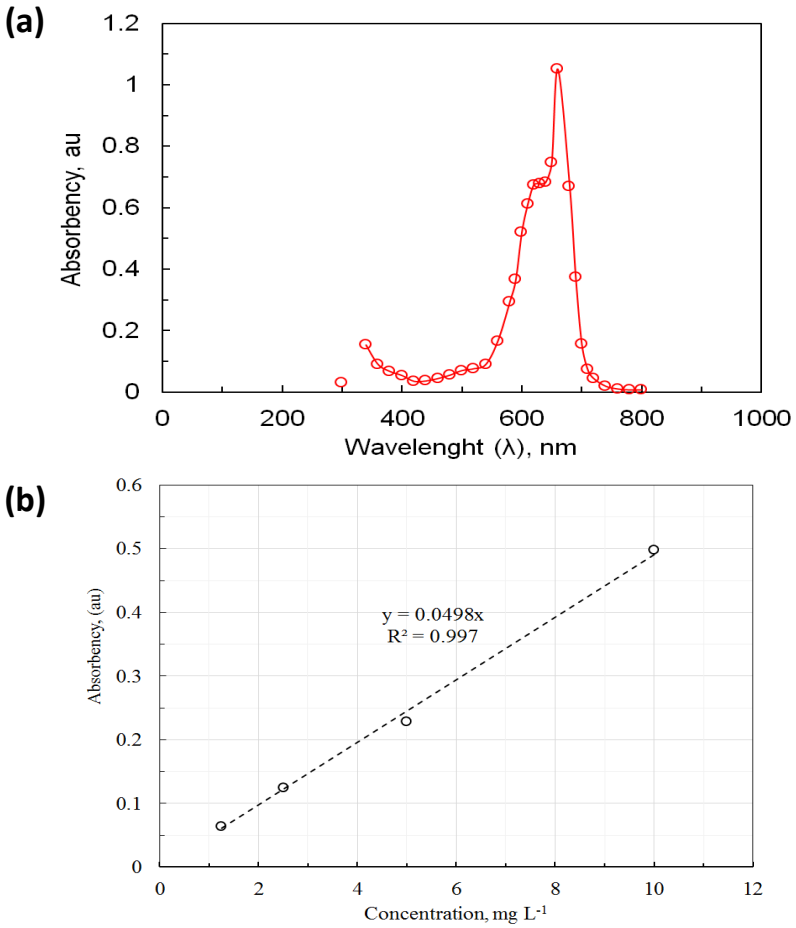

Figure 10. UV-vis results: **(a)** UV-vis spectrum of methylene blue at various wavelength. **(b)** Calibration curve of MB dye.

3.9. Membrane Efficiency

The rejection of methylene blue dye (MBD) from the aqueous solution using the obtained HDPE-based MMMs was experimentally evaluated. Figure 11 shows the MBD rejection efficiency (η%) for each membrane after one hour of processing time (Abushaina *et al.*, 2018). The results indicated that the η% of MBD was increased with an increase in the MC content in the membrane. For example, the η% of neat HDPE membrane was increased from 26.85% to 35.1% with addition HDPE-SC/MC-1. A maximum value of 59.95% of η% was obtained with the sample containing 2% of MC. The increase in the MBD rejection efficiency was ascribed to the fact that MC is rich with the hydroxyl functional groups (-OH) as confirmed using FT-IR results (see Figure 3), which are active cites for adsorption of MBD (Tolba *et al.*, 2016).

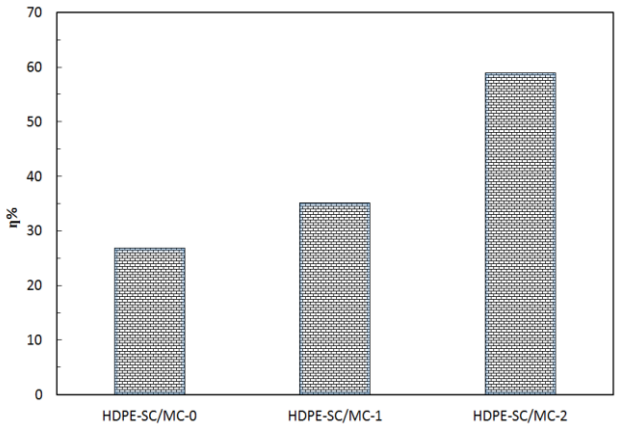

Figure 11. Rejection efficiency of the obtained mixed matric membranes for MBD from aqueous solutions.

3.10. Effect of Processing Time on the Rejection of MBD

The effect of operating time on the rejection efficiency of HDPE-SC/MC-2 membrane was evaluated for 3 h and the results were compared with that obtained using the neat HDPE membrane (HDPE-SC/MC-0). As seen in Figure 12, it was observed that the rejection efficiency values for both membranes were gradually decreased until reached an equilibrium. The results indicated that both samples reached an equilibrium after ~ 40 min processing time. The drop in the MBD rejection efficiency for HDPE-SC/MC-2 with time was smaller than that for the HDPE-SC/MC-0. For example, with an increase in the processing time from 10 to 40 min, the rejection efficiency values of HDPE-SC/MC-0 and HDPE-SC/MC-2 were decreased from 42% to 22% and from 60% to 57%, respectively. This improvement in the removal efficiency may ascribed to the role of MC on the rejection of MD dye via adsorption ability (Tolba *et al.*, 2016).

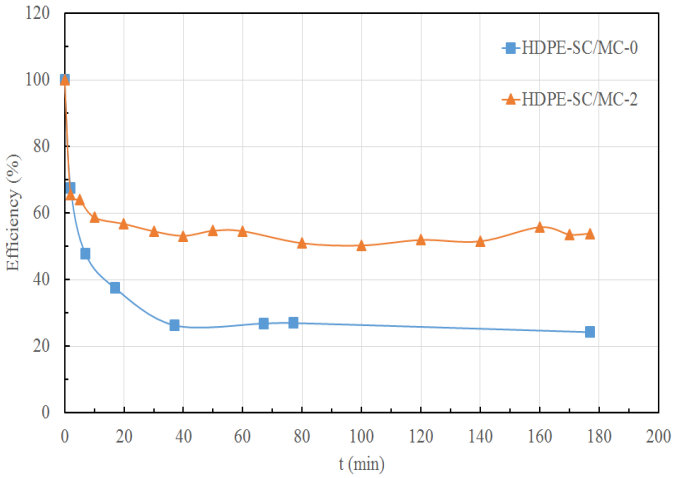

Figure 12. Role of *Mesembryanthemum crystallinum* on the rejection efficiency methylene blue dye.

4. Conclusions

A new type of MMMs were fabricated by thermal method and their characteristics and methylene blue dye rejection performance have been also investigated. The hydrophilicity and porosity of HDPE-based MMMs were increased with addition of MC. In addition, the results of the membranes effluent showed that the modified membranes (HDPE-SC/MC-1, HDPE-SC/MC-2) had higher pure water permeation flux and pore size than that of neat HDPE membrane (HDPE-SC/MC-0). Therefore, the hydrophilicity of MC nanoparticles plays a role on improving the porosity and permeate flux of the MMMs. The maximum permeate flux of 237.52 $L/m^2.h$ was achieved using HDPE-SC/MC-1 mixed matrix membrane. These novel MMMs were tested for the separation of MB dye from aqueous solutions. It was found that the HDPE-SC/MC-2 membrane had better rejection of MB dye molecules as compared to the neat HDPE membrane (HDPE-SC/MC-0). The increase in retention of MB dye was ascribed to the affinity of MC for the adsorption of MB day. Under the optimal conditions, the maximum rejection efficiency of MB dye was obtained are 59.95%. Therefore, we expected that two cycles of MB dye effluent could remove all the dye molecules from the water stream. In besides, this type of MMMs seems to have a promising future in the treatment of aqueous effluents containing MB dye in moderate concentrations.

References

Abushaina, A., Sultan, A., Elhrari, W., and Alhwaige, A. A. (2018). Novel green sorbents derived from *Mesembryanthemum*-based biomass for wastewater treatment applications. *First Conference for Engineering Sciences and Technology (CEST-2018) 25-27 September 2018, Garaboulli, Libya*, 345–354.

Ajari, H., Zrelli, A., Chaouachi, B. and Ponti´e, M. (2019). Preparation and characterization of hydrophobic flat sheet membranes based on a recycled polymer. *International Polymer Processing*, 34(3), 376–382.

Alhwaige, A. A., Ishida, H., and Qutubuddin, S. (2013). Biobased chitosan/polybenzoxazine cross-linked films: preparation in aqueous media and synergistic improvements in thermal and mechanical properties. *Biomacromolecules* 14, 1806−1815..

Alhwaige, A. A., Ishida, H., and Qutubuddin, S. (2019). Poly (benzoxazine-f-chitosan) films: The role of aldehyde neighboring groups on chemical interaction of benzoxazine precursors with chitosan. *Carbohydrate Polymers*, 209, 122–129.

Alhwaige, A. A., Ishida, H., and Qutubuddin, S. (2024). Nitrogen-enriched carbon aerogels derived from polybenzoxazine cross-linked graphene oxide-chitosan hybrid matrix with superior CO_2 capture performance. *ACS Applied Engineering Materials*. 2, 1672−1686

Ekrayem, N. A., Alhwaige, A. A., Elhrari W., and Amer, M. (2021). Removal of lead (II) ions from water using chitosan/polyester crosslinked spheres derived from chitosan and glycerol-based polyester. *Journal of Environmental Chemical Engineering*, 9, 106628.

Ezzeghni, U. A. S., and El-Bourawi, M. S. (2016). Performance improvement and optimization of 10,000 m^3/day SWRO desalination plant. *First International Conference on Chemical, Petroleum, and Gas Engineering (ICCPGE-2016), Alkhoms, Libya*, 1, 25–30.

Figoli, A., and Criscuoli, A. (Eds.). (2017). Sustainable membrane technology for water and wastewater treatment. *Green Chemistry and Sustainable Technology*, 1–66.

Ghaemi, N., and Khodakarami, Z. (2019). Nano-biopolymer effect on forward osmosis performance of cellulosic membrane: High water flux and low reverse salt. *Carbohydrate Polymers*, 204, 78–88.

Ghazanfari, D., Bastani, D., and Mousavi, S. A. (2017). Preparation and characterization of poly (vinyl chloride) (PVC) based membrane for wastewater treatment. *Journal of Water Process Engineering*, 16, 98–107.

Jhaveri, J. H., and Murthy, Z. V. P. (2016). Nanocomposite membranes. *Desalination and Water Treatment*, 57, 26803–26819.

Katare, A., and Mandal, B. (2023). Green-synthesized HF-free MIL-100 (Fe) nanoparticle-infused chitosan mixed-matrix membranes for enhanced CO_2 permeance. *Industral & Engineering Chemical Research*, 62, 11151−11164.

Lin, C. –H., Gung, C. –H., Sun, J. –J., and Suen, S. -Y. (2014). Preparation of polyethersulfone/plant-waste-particles mixed matrix membranes for adsorptive removal of cationic dyes from water. *Journal of Membrane Science*, 471, 1, 285–298.

Liu, C., Ma, Z., Zhang, X., Tang, S., Zhu, Z., He, P., Lei, S., Liu, Z., Wang, T., Wang, Y., and Zhang, S. (2024). Separating 2-phenylethanol from aqueous solution by mixed matrix composite membranes based on beta-cyclodextrin metal organic frameworks. *Separation and Purification Technology*, 330, 125463.

Lloyd, D. R., Kinzer, K. E., and Tseng, H. S. (1990). Microporous membrane formation via thermally induced phase separation. I. Solid-liquid phase separation. *Journal of Membrane Science*, 52(3), 239–261.

Lok, A., Bérubé, P. R., and Andrews, R. C. (2017). The Effect of Concentration Factor on Membrane Fouling. *Membranes*, 7, 50.

Mahajan, R., and Koros, W. J. (2004). Mixed matrix membrane materials with glassy polymers. Part 1. *Polymer Engineering and Science*, 42, 7, 1420–1431.

Nam, Y. S., and Park, T. G. (1999). Biodegradable polymeric microcellular foams by modified thermally induced phase separation method. *Biomaterials*, 20, 1783–1790.

Roy, S., and Singha, N. R. (2017). Polymeric nanocomposite membranes for next generation pervaporation process: Strategies, challenges and future prospects. *Journal of Membrane Technology*, 7(3), 53.

Saedi, S., Madaeni, S. S., Seidi, F., Shamsabadi A. A., and Laki, S. (2013). Synthesis and application of a novel Amino-Starch derivative as a new polymeric additive for fixed facilitated transport of carbon dioxide through an asymmetric polyethersulfone (PES) membrane. *International Journal of Greenhouse Gas Control* 19, 126–137.

Salima, A., Ounissa, K. –S., Lynda, M., and Mohamed, B. (2012). Cationic dye (MB) removal using polymer inclusion membrane (PIMs). *Procedia Engineering*, 33, 38–46.

Strathmann, H., Giorno, L., and Drioli E. (2016). An Introduction to membrane science and technology. *Institute on Membrane Technology CNR-ITM*, 1–3.

Swamy, B. V., Madhumala, M., Prakasham, R. S., and Sridhar. S. (2013). Nanofiltration of bulk drug industrial effluent using indigenously developed functionalized polyamide membrane. *Chemical Engineering Journal*, 233, 193–200.

Tolba, G. M. K., Bastaweesy, A. M., Ashour, E. A., Abdelmoez, W., Khalil, K. A., and Barakat, N. A. M. (2016). Effective and highly recyclable ceramic membrane based on amorphous nanosilica for dye removal from the aqueous solutions. *Arabian Journal of Chemistry* 9, 2, 287–296.

Qu, X., Alvarez, P. J. J., and Li, Q. (2013). Applications of nanotechnology in water and wastewater treatment. *Water Research*, 47, 12, 3931–3946.

Wang, J., Dlamini, D. S., Mishra, A. K., Pendergast, M. T. M., and Wong, M. C. Y. (2014). A critical review of transport through osmotic membranes. *Journal of Membrane Science*, 454, 516–537.

Warsinger, D. M., Chakraborty, S., Tow, E. W., Plumlee, M. H., Bellona, C., Loutatidou, S., Karimi, L., and Mikelonis, A. M. (2018). A review of polymeric membranes and processes for potable water reuse. *Progress in Polymer Science*, 81, 209–237.

Wetzel, G. W. (2001). Limnology: Lake and River Ecosystems. *Academic Press*, New York, 15–42.

Wu, Z., Zeng, J., Huang, X., Zhang, R., and Liu, P. (2023). Mixed matrix membranes with highly dispersed UiO-66-NH_2 filler for removal of dyes and molybdenum (VI) ions from aqueous solutions. *Colloids and Surfaces A: Physicochemical and Engineering Aspects* 674, 31959.

Zheng, X., Zhang, Z., Yua, D., Chena, X., Chenga, R., Mina, S., Wanga, J., Xiaoa, Q., and Wang, J. (2015). Overview of membrane technology applications for industrial

wastewater treatment in China to increase water supply. *Resources, Conservation and Recycling*, 105, 1–10.

Zulfiani, U., Junaidi, A., Nareswari, C., Ibnu Ali, B. T., Jaafar, J., Widyanto, A. R., Saiful, Dharmab, H. N. C., and Widiastuti, N. (2023). Performance of a membrane fabricated from high density polyethylene waste for dye separation in water. *RSC Advances*, 13, 7789–7797.

Zulfiani, U., Pratama, A. W., Abdullah, R., Astira, D., Romadiansyah, T. Q., Widyanto, A. R., Saiful, Jafaar, J., Gunawan, T., and Widiastuti, N. (2024). Improving the performance of HDPE plastic membranes for heavy metal removal by incorporating EVA/PDMS. *Results in Engineering*, 24, 103643.

Zukimin, N. W., Jullok, N., Razi, A. N. M., and Fadzilah, M. H., Teknol H. (2017), Membrane from plastic waste for the treatment of contaminated river water. *Jurnal Teknologi*, 79(1-2), 83–88.